Available online at www.sciencedirect.com
SCIENCE DIRECT®
ELSEVIER
Earth and Planetary Science Letters 214 (2003) 379–394
EPSL
www.elsevier.com/locate/epsl

Magnetic characterisation of present-day deep-sea sediments and sources in the North Atlantic

S.J. Watkins, B.A. Maher *

Centre for Environmental Magnetism, Lancaster Environment Centre, Geography Department, Lancaster University, Lancaster LA1 4YB, UK

Received 25 March 2003; received in revised form 18 July 2003; accepted 18 July 2003

Abstract

The North Atlantic plays a key role in global climate through formation of North Atlantic Deep Water, which drives the thermohaline circulation. To understand past and future climate change, it is essential to understand the processes occurring within the present-day North Atlantic but ocean-wide studies of present-day sediment distribution and sources are relatively sparse. Here, we use magnetic measurements to characterise the surface sediments of the North Atlantic and identify the major climatic and oceanographic controls on their magnetic signatures. The magnetic data, and subsequent cluster analysis, identify distinct spatial patterns of sediment sources and transport pathways. Much of the sedimentary magnetic signal appears to be controlled by detrital inputs, especially of windblown dust, and ice-rafted debris (IRD), with a range of different sources. These sediment transport pathways can be validated by making direct comparison of the sediment magnetic properties with source rocks and soils, and with iceberg trajectory and observation data. The spatial distributions of the IRD-dominated sediments substantiate those mapped previously using lithological tracers, provide additional spatial information on sediment sources and pathways, and suggest that deep water currents are less significant than proposed in controlling present-day sediment mineralogy and distribution. The data form a present-day basis for comparison with glacial-stage IRD and dust distributions, and modes of ocean circulation.

Keywords: North Atlantic circulation; sediment magnetic properties; sediment sources

1. Introduction

The North Atlantic plays a key role in global climate through formation of North Atlantic Deep Water (NADW), which drives the thermohaline circulation and controls the transport of heat polewards from the equator. Palaeoclimate data and ocean/atmosphere circulation models indicate that variability of convective activity in the Nordic and Labrador Seas can result in rapid climate change, on timescales of 1–10^5 years. Any future climatic change may be controlled by, and will certainly affect, the oceanography of the North Atlantic. In order to understand both past and future change, it is essential to

* Corresponding author. Tel.: +44-1524-593169; Fax: +44-1524-847099.
E-mail addresses: sarah.watkins@lancaster.ac.uk (S.J. Watkins), b.maher@lancaster.ac.uk (B.A. Maher).

0012-821X/03/$ – see front matter © 2003 Elsevier B.V. All rights reserved.
doi:10.1016/S0012-821X(03)00422-9

understand the processes occurring within the present-day North Atlantic.

Despite the large number of sediment cores taken in the North Atlantic during the last 40 years, ocean-wide studies of present-day sediment distribution and sources are sparse (e.g. [1,2]). Most previous studies have concentrated on selected Atlantic sub-regions, for example, the NE Atlantic [3], the Nordic Seas [4] and the Kara and Laptev Seas [5]. Kissel et al. [6] have examined sediment properties along the path of NADW. Bond et al. [7] mapped ice-rafted debris (IRD) in the northern North Atlantic, based on petrological analysis of >120 core tops; they identified three distinct IRD sources and sinks based on the percentages of haematite-stained grains, volcanic glass and detrital carbonate.

It is also notable that whilst *palaeo*-oceanographic conditions have been examined in detail (especially, for example, during Heinrich events), a detailed picture of present-day conditions has yet to be defined. For example, IRD is clearly an important sediment source in the polar and sub-polar North Atlantic but the modern-day IRD distribution has yet to be reconstructed over the whole ocean basin [8,9].

This study uses magnetic measurements to characterise the surface sediments of the North Atlantic and identify the major climatic and oceanographic controls on their magnetic signatures. It also aims to provide geological data for ground-truthing of iceberg trajectory models [10]. It directly complements both the study of Schmidt et al. [11], who used the magnetic characteristics of surface sediments to identify major sediment sources and pathways in the South Atlantic, and a similar magnetic data set for a smaller number of North Atlantic surface samples (Robinson, personal communication). Compared with other analytical methods, magnetic measurements have the advantage of being non-destructive, rapid and can be carried out on small ($\sim$1 g) samples, enabling conservation of often scarce surface materials.

The magnetic mineralogy of sediments can reflect distinctive detrital inputs (aeolian, ice-rafted, bottom water-transported), authigenesis via in situ formation of magnetite by magnetotactic bacteria and/or the effects of post-depositional diagenesis. Diagenetic effects can mostly be excluded for these surface sediments, specifically obtained from box cores and trigger weight cores; they are oxic in nature and show no evidence of the presence of iron sulphides. Thus, investigation of these sediments using a number of different magnetic properties may allow identification of the sources and transport pathways of detrital magnetic grains or, in the absence of significant detrital sources, magnetically distinctive, bacterially produced magnetosomes.

To represent the ocean-wide sample area, 321 surface samples have been obtained, through the co-operation of international core archives (see Acknowledgements). In order to identify potential source areas (PSAs), a number of rock, sediment and soil samples were also obtained from the circum-Atlantic region and their magnetic signatures compared directly with the sediments.

Individual magnetic parameters such as magnetic susceptibility can be affected both by variations in the concentrations of magnetic minerals and/or by the effects of biogenic dilution (e.g. by diamagnetic carbonate). Measurement of magnetic susceptibility (at more than one frequency) and an additional range of magnetic remanence parameters enable calculation of a number of interparametric ratios, in which such concentration and/or dilution effects are removed. Given there may be possible overlap between sample magnetic properties (perhaps reflecting mixing of different magnetic sources), multivariate methods of analysis are appropriate. Fuzzy c-means cluster analysis is used here, as applied recently to a number of different environmental data sets, including: magnetic mapping of pollution in soils [12], analysis of the climatic/magnetic connections for sediments from the Azores region [13], and the previously cited magnetic study of surface sediments in the South Atlantic [11].

2. Samples and methods

Core locations for the 321 North Atlantic samples are shown in Fig. 2 (and following). Surface samples were mostly obtained from box and trig-

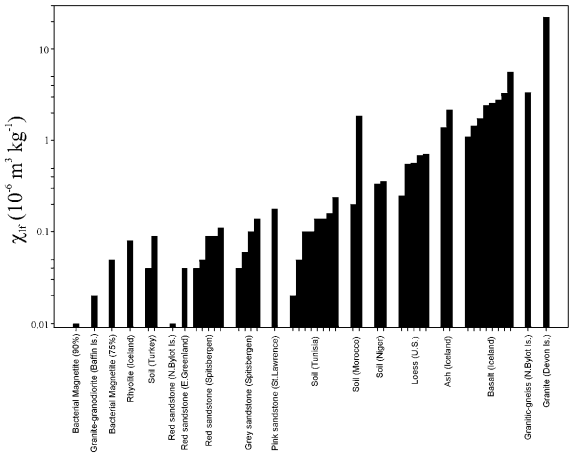

Fig. 1. Bar chart showing susceptibility data (χ_{lf}, $\times 10^{-6}$ m^3 kg^{-1}) for measured PSA samples.

ger weight cores (piston core samples were only used when comparison of the piston and trigger weight core indicated surface sediment was present in both). Samples from PSAs were also collected, including: soils from the North African region; Icelandic basalts and volcanic ash; Devonian and Triassic redbeds from Spitsbergen and east Greenland, respectively; Caribbean carbonates containing bacterial magnetite; granites from north Bylot Island; and a range of other lithologies from the circum-Atlantic area (Fig. 1). Wet samples were dried overnight at 40°C and sample weights measured to allow for correction of measurements to a dry mass-specific basis. Samples were firmly packed, to avoid internal movement of the sample within the holder, into 10-cc plastic pots. A suite of susceptibility and remanence measurements was applied to all samples with the aim of characterising their magnetic mineralogy, concentration and magnetic grain size (domain state). All fields were applied and remanences measured along the same axis. The Appendix details the instrumentation used. In order to remove variations caused by changes in magnetic concentration (due to possible biogenic dilution and/or variations in sedimentation rates), normalised, interparametric ratios were calculated from the susceptibility values (measured at low and high frequencies) and the anhysteretic and remanent magnetisations. Carbonate values were obtained, either as published values or interpolated from the data of Balsam and McCoy [1], for 60% of the sample set and spanning the whole measured susceptibility range. Geographic plots of the magnetic data were generated using ArcView, each sample point being represented by a shaded area of 300 km radius.

Given the reasonably large, multi-parameter magnetic data set produced from the sediment and source samples, univariate or bivariate analysis of individual magnetic parameters may be ineffective in discriminating between possible sediment sources and any mixing between sources. To provide such information, multivariate methods are required. Two multivariate methods are applied here: fuzzy c-means clustering and non-linear mapping, using the program of Vriend et al. [14] in which the clustering algorithm was adapted from Bezdek et al. [15] and the non-linear mapping algorithm based on Sammon [16]. In traditional clustering methods (hierarchical and k-means), a sample is forced to belong to an individual cluster. This may be a disadvantage for this magnetic data set, where a number of processes may be responsible for the magnetic signal and source mixing is a possibility. Fuzzy clustering does not force a sample to belong to a specific cluster; instead, it calculates a membership value, ranging from 0 (no similarity) to 1 (identical), for each sample to each cluster. Following Hanesch et al. [12], samples are classified here as 'belonging' to a cluster, if the ratio of the highest membership to the second highest membership is greater than 0.75; if this condition is not satisfied, the sample is unclassified. This method does not require the number of clusters to be known before clustering and the program iteratively performs the clustering for two to nine clusters. The 'best' solution is calculated by minimising the distance between a sample and its cluster centre and maximising the distance between the cluster centres [13]. These distances are represented by two statistics produced by the program: the partition coefficient F and the classification entropy H. The 'best' number of clusters is given by the highest F and lowest H value [12]. Non-linear mapping, a multidimensional scaling method [12], was also used to evaluate the results of the fuzzy c-means cluster-

ing [17]. It provides a means of plotting the multi-dimensional relationship between samples and clusters in two dimensions.

Fuzzy clustering was run using the following magnetic parameters: (a) the high-field remanence (the HIRM, as a percentage of the saturation remanence, SIRM), to identify the presence of the high-coercivity minerals, haematite/goethite; (b) frequency-dependent magnetic susceptibility (χ_{fd}), to identify ultrafine-grained ($< \sim 20$ nm), superparamagnetic (SP) ferrimagnets, such as magnetite and maghaemite; (c) the ratio of the anhysteretic remanence normalised to magnetic susceptibility (χ_{ARM}/χ_{lf}), to identify fine-grained (~ 30–50 nm), single-domain (SD) ferrimagnets; and (d) the 'soft' remanence fraction, i.e. that acquired at the relatively low magnetic field of 20 mT (the $IRM_{20\,mT}/IRM_{100\,mT}$), to identify low-coercivity, multidomain (MD)-like ferrimagnets. Prior to cluster analysis, the magnetic parameters were investigated using the non-parametric Spearman test to ensure that they were not autocorrelated.

All parameters except HIRM% were found to have a log-normal distribution and were thus log-transformed. Nine outliers were identified (values more than three times the standard deviation from the mean value, normal or logarithmic depending on the parameter distribution) and removed from the data set to preclude undue influence on the clustering, leading to unrealistic groupings [12]. Finally, values were standardised so that parameters with large values and/or variability again did not predominate.

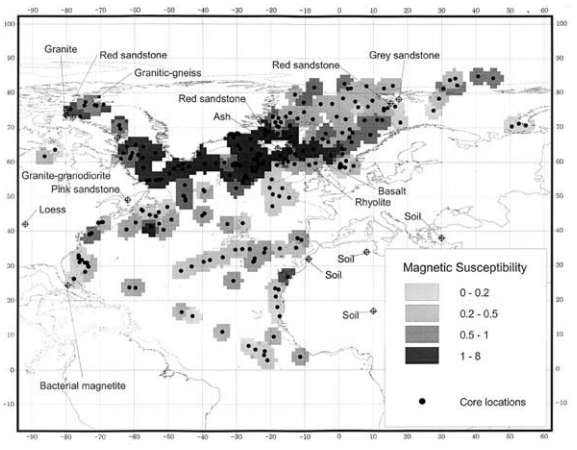

Fig. 2. Geographic distribution of susceptibility (χ_{lf}, $\times 10^{-6}$ m^3 kg^{-1}) in present-day North Atlantic deep-sea sediments (sample values interpolated to 300 km radius of sample site, using ArcView); the locations of the PSA samples are also shown.

3. Results

First, we use ArcView to display the interpolated geographic distributions of the measured magnetic parameters and ratios (Figs. 2, 4, 6 and 8) and then show the results of multivariate statistical analysis of the non-concentration-dependent, sediment magnetic properties.

3.1. Magnetic susceptibility

Magnetic susceptibility provides an indication of how magnetic a sample is:

$$\text{Susceptibility } (\chi_{lf}) = \chi_f + \chi_p + \chi_a + \chi_d$$

where χ_f is the strong, positive susceptibility contributed by ferrimagnets (like magnetite), χ_p and χ_a the weak, positive susceptibility carried by paramagnets (like clay minerals) and high-coercivity minerals (like haematite and goethite), respectively, and χ_d the weak, negative susceptibility of diamagnets (like calcium carbonate). Susceptibility thus often reflects the concentration of ferrimagnets within a sample. Magnetic susceptibility values for our sampled range of potential sources mostly vary from 0.01 to 3.3×10^{-6} m^3 kg^{-1}, with one extreme value of $\sim 23\times10^{-6}$ m^3 kg^{-1}, measured on a granite from Devon Island (Fig. 1). Highest values are associated with the igneous rock samples (basalts and granites) and low values with the African soils, Triassic and Devonian sandstones and carbonate-rich sediments dominated by bacterial magnetite. In comparison, magnetic susceptibility values for the North Atlantic surface sediments were found to range from 0.01 to 8×10^{-6} m^3 kg^{-1} (Fig. 2). The susceptibility data identify a major contrast in present-day North Atlantic sediments and sources. The low-latitude zone, extending in a trans-Atlantic belt west and northwest from Africa

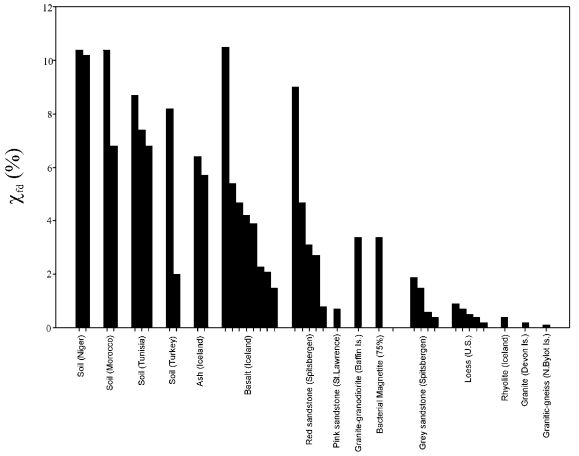

Fig. 3. Bar chart showing frequency-dependent susceptibility (χ_{fd}, %) for PSA samples.

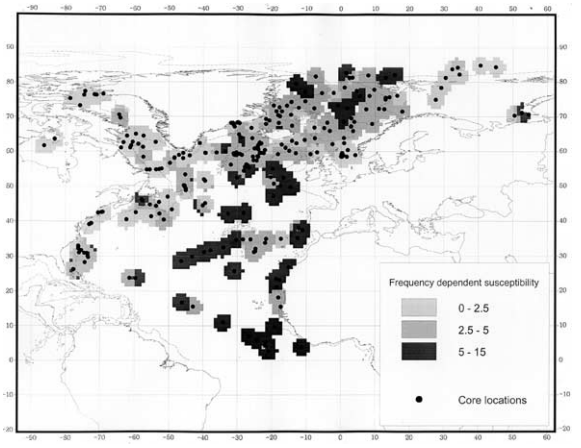

Fig. 4. Geographic distribution of frequency-dependent susceptibility (χ_{fd}, %) in present-day North Atlantic deep-sea sediments (sample values interpolated to 300 km radius of sample site, using ArcView).

(from 0 to ~30°N and to ~60°W), displays the uniformly lowest susceptibility values ($<0.5\times10^{-6}$ m^3 kg^{-1}). This pattern persists even when adjustment of the susceptibility data is made for carbonate content. In contrast, the middle to higher latitudes exhibit much higher and more variable susceptibility values (up to $\sim8\times10^{-6}$ m^3 kg^{-1}). High values ($1–6\times10^{-6}$ m^3 kg^{-1}) are found all around Iceland, possibly associated with: (a) the underlying, magnetite-rich basalt of the mid-ocean ridge and the Iceland–Faeroe ridge (Fig. 1); (b) movement of sediment in the South Iceland Basin by Iceland–Scotland Overflow Water (ISOW), a component of NADW; and (c) possible deposition of sub-aerially erupted ash (Fig. 1). Additional high-susceptibility locations include sites off the east Greenland coast, coinciding with the location of major iceberg-calving glaciers. Intermediate values occur in the Labrador Sea, Baffin Bay and to the south of Greenland and are also probably associated with iceberg rafting. Maximum rates of iceberg melting off eastern Canada occur presently in the Labrador Current at 54–50°N [18]. It is also possible that there has been some subsequent redistribution of IRD by turbidite activity or deep-ocean currents (see below). Within the mid- to high-latitude belt of high susceptibility values, there are localised regions of slightly lower values, including: off Newfoundland; south of Spitsbergen; the eastern Nordic Seas; and southwest of Ireland. In contrast with the South Atlantic [12], no relationship appears to exist between water depth and magnetic susceptibility; shallow pelagic sites show no obvious link with lower susceptibility values. The North Atlantic seems dominated magnetically by distinctive terrigenous inputs rather than by productivity variations.

These terrigenous inputs become more clearly defined upon inspection of the frequency-dependent susceptibility, which displays an almost inverse relationship to susceptibility. Values of fre-

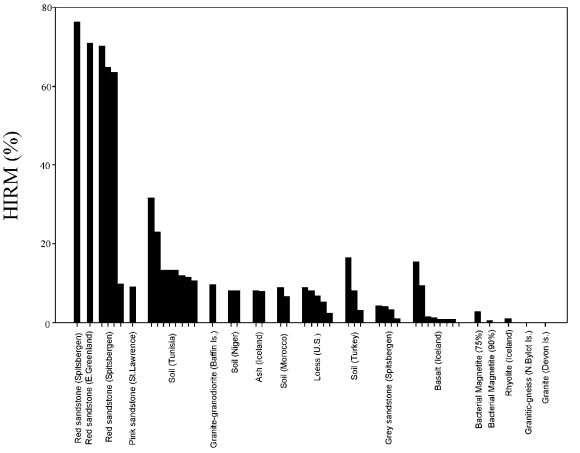

Fig. 5. Bar chart showing HIRM (%) for PSA samples.

quency-dependent susceptibility for the PSAs range from 0.1 to 10% (Fig. 3), with maximum values associated with the Niger and Moroccan soil samples and minimum values with acid igneous rocks from Baffin, Devon and north Bylot Islands and the unweathered Illinoian (USA) loess. Values for the North Atlantic sediments range from 0 to ~14% (Fig. 4). Again, the low-latitude belt is distinctive and conspicuous, with two 'plumes' of sediment with the lowest susceptibility and the highest χ_{fd} values – to the west and northwest of the African continent, extending to 50°W and 55°N. Values of χ_{fd} as high as ~14% indicate the dominant presence of ultrafine, SP ferrimagnetic grains, i.e. < ~30 nm in magnetite [19,20]. These two swathes of present-day sediment are thus characterised by low concentrations of dominantly SP ferrimagnets. In contrast, the regions of high and intermediate susceptibility around Iceland, Baffin Bay, the Labrador Sea and along the coast of Greenland are associated with low χ_{fd} values (<4%), indicating the dominance of coarser SD to MD ferrimagnets. The low-susceptibility region in the eastern Nordic Seas is associated with moderate frequency dependence of ~4–8%.

3.2. Magnetic remanences

Remanence ratios can be used to characterise the magnetic stability of samples (e.g. [21]). The relative abundance of the high-coercivity, magnetically 'hard' minerals, haematite and goethite, is indicated by the HIRM (the remanence acquired in fields between 0.3 and 1 T, as a percentage of the total remanence). HIRM values for the PSAs range from 0 to 76%. The highest HIRMs are exhibited by the red sandstones, the lowest by the granitic and basaltic samples (Fig. 5). Values for the North Atlantic surface sediments range from 0.3 to 27% (Fig. 6). The region of highest HIRM% values coincides with the low-susceptibility/high-frequency-dependence belt between 0 and 30°N to the west of Africa (Fig. 6). Well-drained, oxic soils in humid to sub-humid tropical regions form haematite and goethite [22]. Haematite/goethite input to lower-latitude North Atlantic sediments has thus been associated with aeolian transport of such soils from the sub-Saharan/Sahel region of Africa (e.g. [2,23,24]). In addition to this dust-dominated belt, high HIRM values (~10%) are also found close to the eastern coast of North America, between 40 and 50°N. Whilst these values might reflect some distal dust input, it seems more likely that they result from (glacial) erosion of the redbeds in the St. Lawrence region (e.g. [2,25]) transported southwards by the Deep Western Boundary Current [18]. Smaller, localised regions of high HIRM values also occur off the coast of eastern Greenland (at ~70°N) and to the north and northeast of the UK. The high eastern Greenland values may result from the transport of IRD from Triassic redbeds in the Fleming Fjord region (Fig. 5; [26]). Redbeds of Devonian age are found in the central peninsula of northern Spitsbergen (Fig. 5); the intermediate HIRM values (6–8%) found in the eastern Nordic Seas may similarly be the result of transport of haematite-rich IRD. Other regions, including Baffin Bay, the Labrador Sea and the coast of Greenland south of ~65°N, are characterised by lower HIRM values (<6%), indicating domination by ferrimagnets.

Another remanence ratio, identifying the proportion of remanence acquired at low applied fields (here, $IRM_{20\,mT}$, normalised to the remanence acquired at 100 mT), can act as an indicator of ferrimagnetic grain size (domain state).

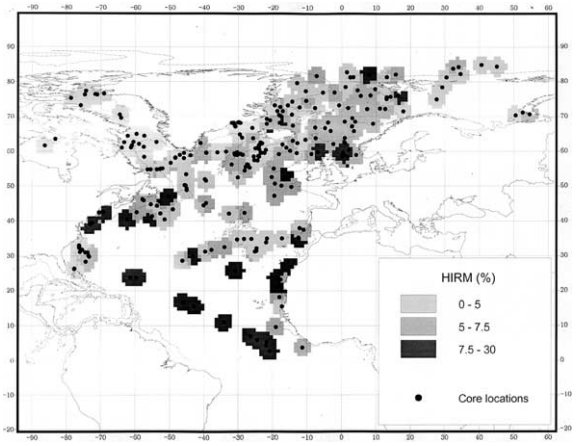

Fig. 6. Geographic distribution of HIRM (%) in present-day North Atlantic deep-sea sediments (sample values interpolated to 300 km radius of sample site, using ArcView).

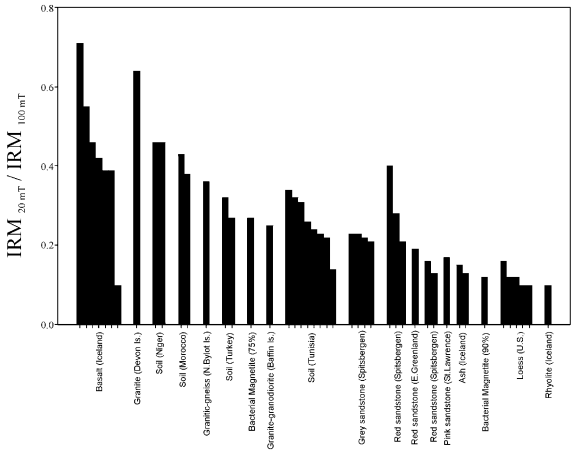

Fig. 7. Bar chart showing the proportion of remanence acquired at low applied fields ($IRM_{20\,mT}/IRM_{100\,mT}$) for PSA samples.

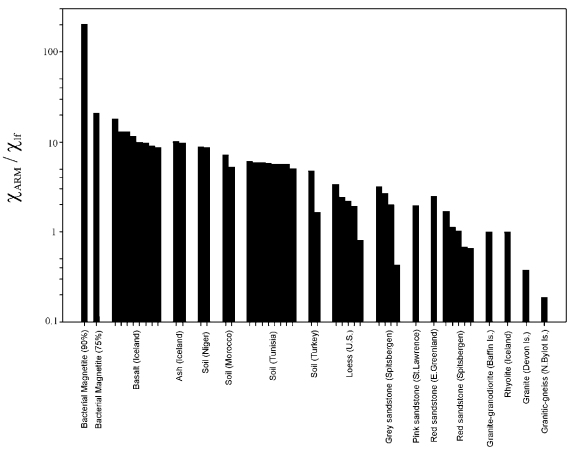

Fig. 9. Bar chart showing χ_{ARM}/χ_{lf} ratios for PSA samples.

High values of this parameter indicate higher amounts of ferrimagnets that are easy to magnetise, i.e. either coarse MD or viscous grains on the SD/SP border. Values of this low-field remanence ratio for the PSA samples (Fig. 7) range from maxima of ~0.5–0.7 for the Niger and Moroccan soils and the basalt samples, to a minimum of 0.1 for the US loess samples and the purest (carbonate+) bacterial magnetite sample. For the North Atlantic sediments (Fig. 8), $IRM_{20\,mT}/IRM_{100\,mT}$ values range from 0.01 to 0.56. Highest values are found between the equator and 40°N, extending to ~50°W. As this corresponds to the 'dust belt' region of low susceptibility, high frequency dependence, high HIRM and intermediate to high χ_{ARM}/χ_{lf}, it is likely that the high $IRM_{20\,mT}/IRM_{100\,mT}$ ratio indicates here the presence of viscous SD/SP grains. The region surrounding Iceland is characterised by intermediate values, most likely associated with the basaltic ridge material (Fig. 7). Lowest values are found in Baffin Bay and in parts of the Labrador Sea and close to the southern coast of Greenland. Given the high sus-

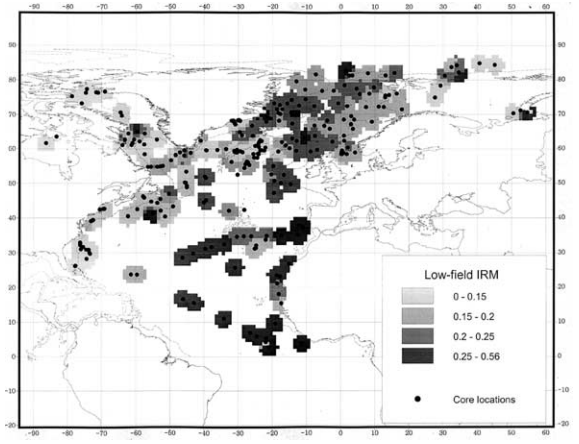

Fig. 8. Geographic distribution of low field remanence ($IRM_{20\,mT}/IRM_{100\,mT}$) in present-day North Atlantic deep-sea sediments (sample values interpolated to 300 km radius of sample site, using ArcView).

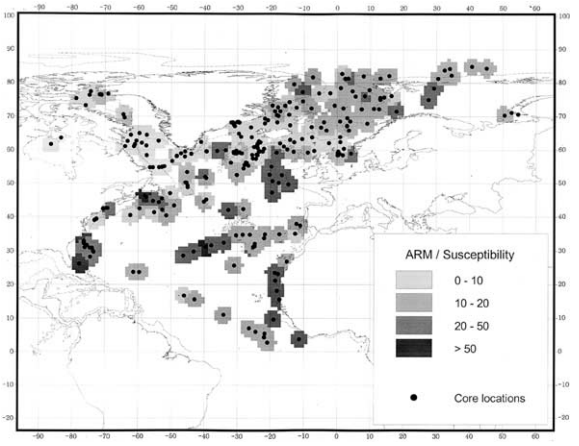

Fig. 10. Geographic distribution of χ_{ARM}/χ_{lf} ratios in present-day North Atlantic deep-sea sediments (sample values interpolated to 300 km radius of sample site, using ArcView).

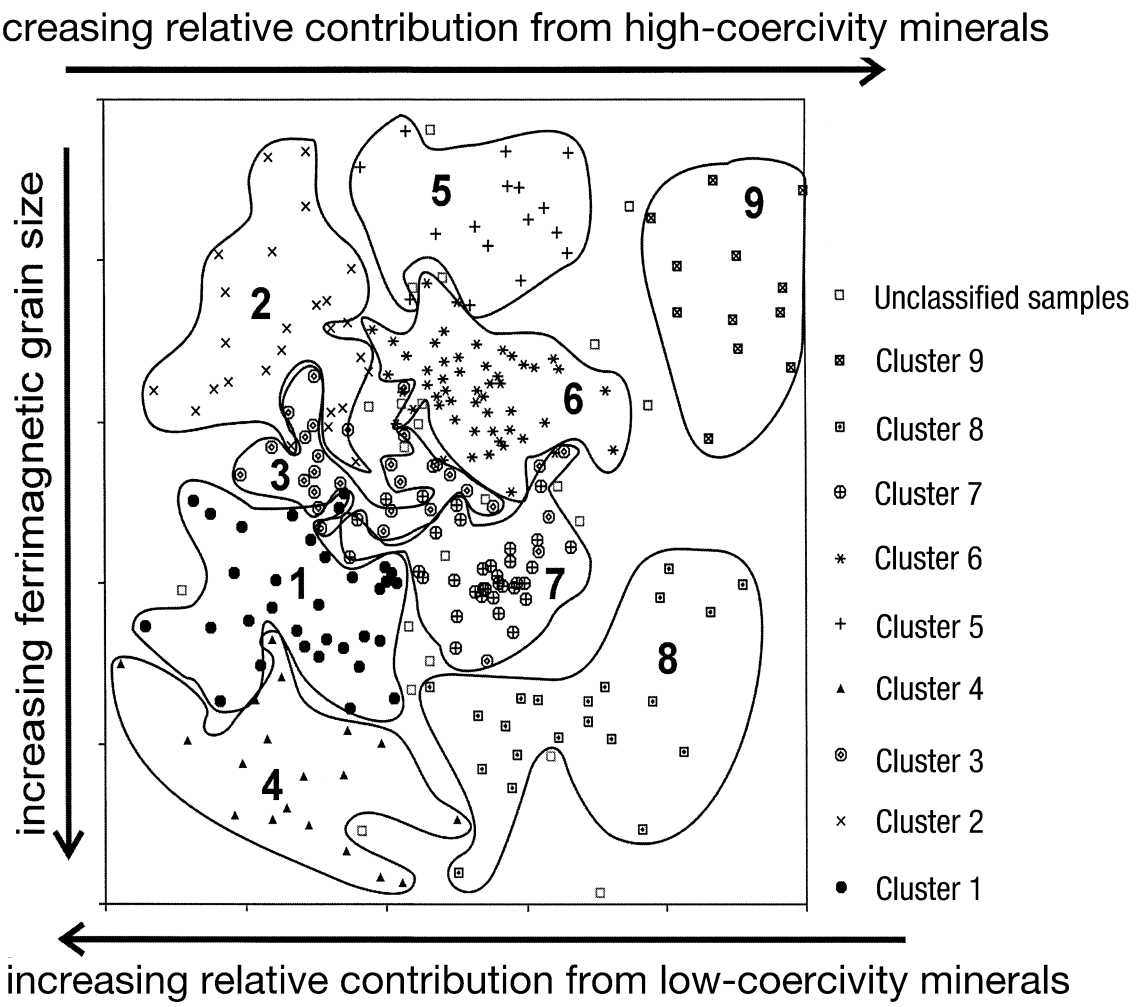

Fig. 11. Summary of the non-linear mapping for the nine-cluster solution.

ceptibility, low frequency dependence and low HIRM of these samples, these low-$IRM_{20\,mT}$/$IRM_{100\,mT}$ areas probably reflect the presence of lithogenic SD/PSD ferrimagnets. There is also a region of low $IRM_{20\,mT}/IRM_{100\,mT}$ values off the eastern North American coast. These low values coincide with low χ_{lf}, χ_{fd}, and HIRM values and high χ_{ARM}/χ_{lf} values, suggesting the presence of SD ferrimagnets of bacterial magnetite origin (see below).

Finally, the susceptibility of ARM (χ_{ARM}) is highest for strongly interacting SD ferrimagnets (such as the ferrite chains produced intracellularly by magnetotactic bacteria) and decreases rapidly with increasing grain size (e.g. [19,27]). Normalising χ_{ARM} with susceptibility (χ_{lf}), to remove magnetic concentration effects, values for the PSAs range from 0.2 to 204 (Fig. 9), with the carbonate sample containing intact bacterial magnetite displaying the highest value and the red sandstones and igneous rocks the lowest. The χ_{ARM}/χ_{lf} values for the North Atlantic surface sediments are very similar in range to the measured PSAs, from 0.5 to 254 (Fig. 10). Maximum χ_{ARM}/χ_{lf} values are found in restricted areas close to the southeastern coast of North America

(~30°N), south of Newfoundland, the African coast and west of the UK. The highest values (>50) occur in association with low susceptibility, HIRM and $IRM_{20\,mT}/IRM_{100\,mT}$ values, indicating little detrital input of source materials such as either dust or IRD. We infer the dominant presence of intact, SD, bacterial magnetite chains (e.g. [28–30]) formed in situ in these areas. Less extreme values (20–50) off the southeastern coast of North America may be linked to the presence of broken bacterial magnetite chains. Values in the range 20–50 are also found for sediments to the west of Africa, together with high χ_{fd} and $IRM_{20\,mT}/IRM_{100\,mT}$ ratios, indicating the presence of SD, SD/SP and SP ferrimagnets. Such grain size assemblages are characteristic of soil-formed ferrimagnets [27,31]. Minimum χ_{ARM}/χ_{lf} values are observed along the eastern coast of Greenland, around Iceland, Baffin Bay and the Labrador Sea, indicating for each of these regions the contribution of coarser, MD-like ferrimagnets. Intermediate values of χ_{ARM}/χ_{lf} (10–20) are associated with the 'dust belt' regions of low susceptibility and high χ_{fd} and HIRM to the west and northwest of the African continent. A region of intermediate values also surrounds Spitsbergen.

4. Discussion

Geographic presentation of the individual magnetic properties of the North Atlantic surface sediments reveals evidence of areal differentiation and distinctive terrigenous (dominantly) and authigenic magnetic sources. To integrate the magnetic data and make objective identification of sediment groupings and transport pathways, multivariate analysis is required. Only parameters independent of magnetic mineral concentration were used in the fuzzy cluster analysis applied here. Compared with the sediments, many of the potential source samples display magnetic parameter values which fall as outliers, and so cannot be included as end-members. Mixing of sources is thus indicated; mathematical unmixing of sediments in terms of sources is the subject of further analysis and will be reported in a later paper.

The statistical indicators of cluster performance, highest F and lowest H, suggest that the 'best' clustering solution for the magnetic data set for the North Atlantic present-day sediments is achieved with nine clusters. The parameter means for each of these nine clusters are shown in Table 1. Fig. 11 shows the results of the non-linear mapping (NLM) of the data. Making no presumptions regarding the presence or number of clusters, the NLM displays a two-dimensional projection of the multidimensional data cloud, with minimal distortion of the interdata distances [14]. Six of the nine clusters are well separated (i.e. display large interdata distance): clusters 1, 2, 4, 5, 8 and 9. The three remaining clusters, 3, 6 and 7, are well-defined, but separated by smaller distances, and fall in the central part of the NLM. Samples dominated magnetically by fine-grained ferrimagnets (cluster 2) plot in the upper left section of the NLM. Further to the right, samples become increasingly dominated by high-coercivity behaviour (cluster 5 to cluster 9). In contrast, sediments dominated by coarse ferrimagnets (clusters 1, 4, 7, 8) plot in the lower section of the NLM. These are further split into clusters by variations in their concentration of high-coercivity minerals. Samples plotting towards the middle

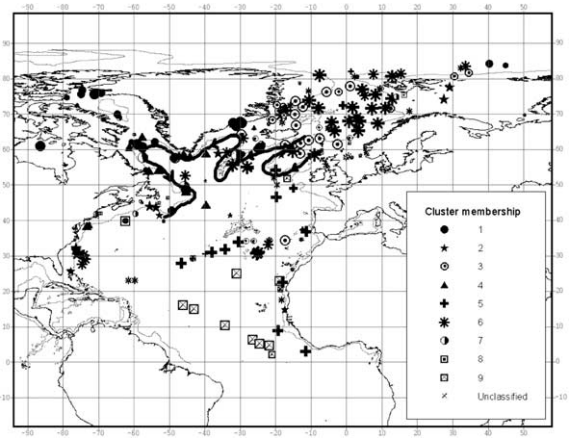

Fig. 12. Geographic distribution of the magnetic nine-cluster solution, based on 276 sediment samples (i.e. excluding those with missing magnetic values). Twenty-two samples were unclassified, i.e. 8% of the sample set. The symbol size represents the degree of affinity with each cluster. The solid line represents the approximate path of the NADW.

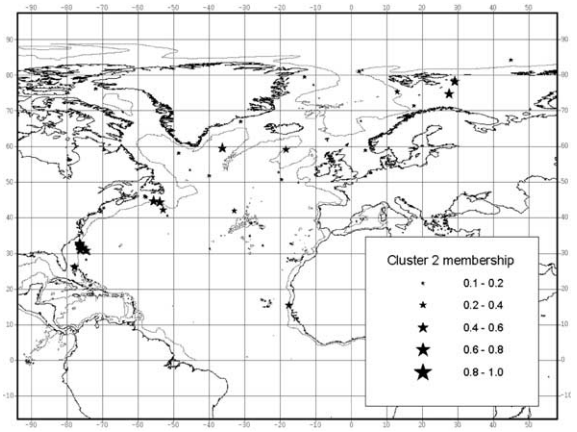

Fig. 13. Location of samples belonging to cluster 2 (dominated by bacterial magnetite). The symbol size represents the degree of affinity with the cluster.

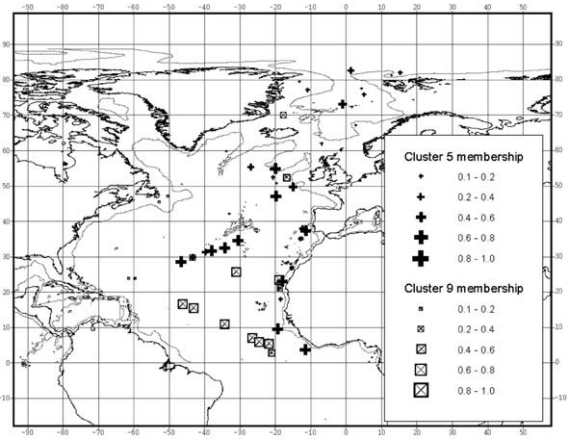

Fig. 14. Location of samples belonging to clusters 5 and 9 (dominated by wind-blown dust). The symbol size represents the degree of affinity with the cluster.

of the NLM (clusters 3, 6, 7) interface between the coarse- and fine-grained clusters, most likely indicating a mixture of sources. Fig. 12 shows the spatial distribution of all the cluster results. No information on the spatial distribution of samples is included in the fuzzy c-means cluster analysis. Hence, the distinctive spatial groupings that result are notable.

4.1. Cluster 2

Samples with strong affinities to cluster 2 are found close to the coast in two main regions: (a) off the southeast coast of the southern USA (~30°N) and (b) in a narrow transect extending southeast from the Gulf of St. Lawrence (Fig. 13). Additional, single samples belonging to this cluster are distributed throughout the North Atlantic (e.g. off the African coast at ~16°N; south of Iceland; southeast of Greenland; and east of Spitsbergen). The cluster means indicate the dominance of SD ferrimagnets, with the highest χ_{ARM}/χ_{lf} values (39), low HIRM (3.4%) and low χ_{fd} (3%). Given that susceptibility values are also low in these regions, little detrital input is indicated but rather the predominance of bacterial magnetite, formed in situ. Intact magnetosome chains are characterised by high χ_{ARM} and low χ_{fd} values (e.g. [29,32]). The slightly higher HIRM of this cluster in comparison to our measured bacterial magnetite representatives may result from a contribution of either windblown dust [2] or glacially derived haematite, transported from the St. Lawrence redbeds region by the Deep Western Boundary Current. It is likely that bacterial magnetite formation occurs in surface sediments right across the North Atlantic at the present day but is only identified as the major magnetic component when detrital inputs are minimal.

Table 1

	Cluster 1	Cluster 2	Cluster 3	Cluster 4	Cluster 5	Cluster 6	Cluster 7	Cluster 8	Cluster 9
HIRM (%)	2.97	3.45	4.64	4.32	5.58	5.68	6.23	8.26	10.61
χ_{ARM}/χ_{lf}	6.73	39.04	8.58	2.78	25.43	16.69	9.26	5.24	15.87
$IRM_{20\,mT}/IRM_{100\,mT}$	0.11	0.13	0.22	0.16	0.26	0.18	0.11	0.10	0.35
χ_{fd} (%)	2.10	2.97	2.48	0.78	7.64	4.13	3.59	1.53	7.63

4.2. Clusters 5 and 9

Samples belonging to cluster 5 and cluster 9 are found south of 60°N in two bands: the first extending northwest and the second west from Africa. Both clusters have distinctive and similar magnetic properties (Fig. 14). They have the highest χ_{fd} means (~8%). Cluster 9 also has the highest HIRM mean (11%). The potential source materials measured here, i.e. topsoils from Morocco, Tunisia and Niger, match strongly with these sediment magnetic properties and have strong statistical affinity (>0.8) with these clusters. The only exception is that the sediments have slightly higher χ_{ARM}/χ_{lf} values; a minor magnetic contribution of ~2–10% intact bacterial magnetosomes could account for this difference.

4.3. Clusters 1, 4, 7 and 8

Samples belonging to cluster 1 are mostly restricted to the northwestern North Atlantic (Fig. 15), being located in Baffin Bay and the northwestern Labrador Sea. Additional cluster 1 samples occur off the coast of east Greenland at ~70°N, southwest of Iceland and one sample north of Spitsbergen. χ_{fd} and χ_{ARM}/χ_{lf} are both low (Table 1) and HIRM% is the lowest for any of the clusters. These data indicate the dominance of MD ferrimagnets. Large numbers of cluster 1 samples are located close to present-day calving glaciers. The geology surrounding these sites is dominated by (titano)magnetite-rich, Precambrian acid igneous rocks and Tertiary basalts. Ice-rafting is thus the most likely sediment transport mechanism for these sites. For more proximal sites, debris flows and turbidites may also be significant sediment sources (e.g. the nearshore northwestern Labrador Sea [33]). IRD in north Labrador Sea samples most likely derives from icebergs released around Baffin Bay, where the dominant geology is Precambrian granite and gneiss. The geographic distribution of these cluster 1 samples closely matches the IRD source (Baffin Bay) and deposition area (Labrador Sea) mapped lithologically by Bond et al. [7] on the basis of the presence of detrital carbonate (>10%). However, cluster 1 samples extend further eastwards than inferred by these authors.

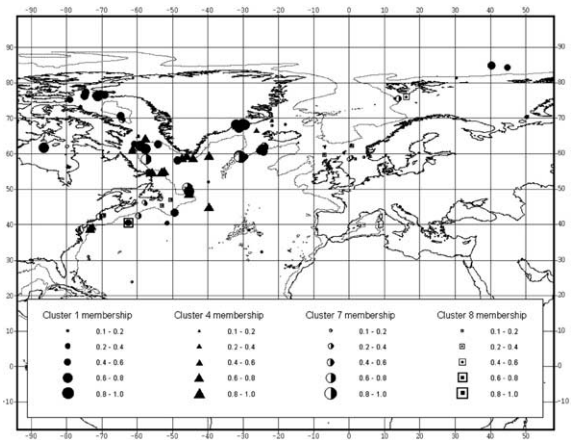

Fig. 15. Location of samples belonging to clusters 1, 4, 7 and 8 (dominated by IRD). The symbol size represents the degree of affinity with the cluster.

IRD sources for the cluster 1 samples off east Greenland mostly comprise granodioritic gneisses and granite, with Triassic redbeds further north. Our potential source rock sample (granitic gneiss from north Bylot Island) provides an obvious source of coarse, MD ferrimagnets, being characterised by high susceptibility (3×10^{-6} m^3 kg^{-1}), minimal χ_{fd} (<1%), zero HIRM% (saturated by 300 mT), and a high $IRM_{20\,mT}/IRM_{100\,mT}$ value of 0.36. As these magnetic values are more extreme than the cluster 1 means, some subsidiary admixture of other sources is likely (e.g. bacterial magnetite (~3%) to raise the χ_{ARM}/χ_{lf} and red sandstone (~4%) to raise the HIRM). A mix of 40% granitic gneiss and 60% Icelandic ash also produces values comparable to, but slightly higher than, the cluster 1 means.

The cluster 1 samples south of Iceland lie along the eastern flank of the mid-Atlantic ridge and probably result from bottom water transport by ISOW. Whilst they have highest affinity with cluster 1, they also display some affinity with cluster 7, which appears to have a significant contribution from Icelandic ash as a source material.

Cluster 4 samples are mainly restricted to the northwestern North Atlantic, off the southern Greenland coast and in the Labrador Sea (Fig. 15). This cluster has the lowest χ_{fd} (0.8%) and

χ_{ARM}/χ_{lf} (2.8) values, indicating the dominance of coarse MD ferrimagnets. Both the geographic extent and cluster means of cluster 4 are similar to cluster 1; a similar, IRD contribution is indicated for most of these samples. Samples at 40°N, along the US coast, may appear too proximal to result from IRD, but the International Ice Patrol reports modern iceberg sightings as far south as 38°N [34].

Cluster 7 samples are found in similar regions to clusters 1 and 4, again suggesting an IRD source. However, an additional cluster 7 group lies south of Iceland, along the mid-Atlantic ridge. Cluster 7 has a higher contribution from high-coercivity minerals (HIRM = 6.2%) and SP ferrimagnets (χ_{fd} = 3.6%). Low values of χ_{ARM}/χ_{lf} (9) and $IRM_{20\,mT}/IRM_{100\,mT}$ (0.1) suggest the presence of PSD-type grains. The cluster means correspond well with our Icelandic ash samples (although these have slightly higher χ_{fd} values). It is possible, therefore, that this group reflects transport and deposition by the bottom water currents of the ISOW [6].

Cluster 8 is restricted to two small regions, off Newfoundland/Nova Scotia, and south of Spitsbergen. The HIRM values (8%) indicate significant contribution by high-coercivity minerals. Additionally, however, χ_{fd}, χ_{ARM}/χ_{lf} and $IRM_{20\,mT}/IRM_{100\,mT}$ values are all low (1.5%, 5 and 0.10, respectively) indicating coarse ferrimagnets, of likely IRD origin. The Newfoundland/Nova Scotia region of high HIRM values may be associated with the glacially derived redbed sediments, redeposited by turbidity or bottom currents, offshore from the St. Lawrence region [2,18]. The high HIRMs north of Norway may be related to ice-rafting from Devonian redbeds on Spitsbergen.

In summary, most of the samples belonging to the IRD clusters substantiate Bond et al.'s [7] conclusion that most (tracer-bearing) ice circulates in the cooler waters north and west of the subpolar front. Whereas Bond et al. [7] inferred the presence of IRD from south and west Greenland on the basis of low tracer percentages, the cluster data presented here identify IRD from these source regions both to the south of Greenland and in the Labrador Sea.

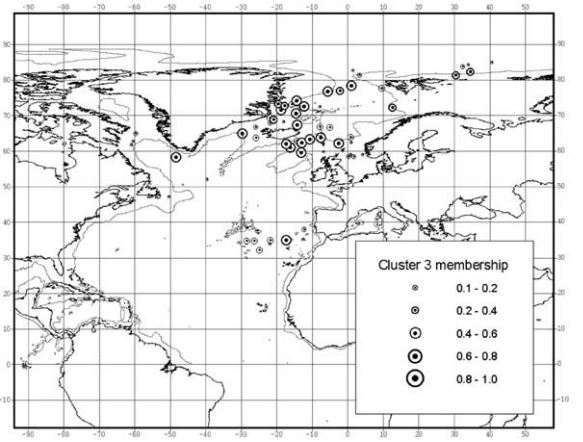

Fig. 16. Location of samples belonging to cluster 3 (mid-ocean ridge and volcanic material). The symbol size represents the degree of affinity with the cluster.

4.4. Cluster 3

Parameter means for cluster 3 indicate MD ferrimagnets (low χ_{ARM}/χ_{lf} and χ_{fd} and slightly higher $IRM_{20\,mT}/IRM_{100\,mT}$ and HIRM values than the cluster 1 samples). Notably, most samples are located around Iceland (Fig. 16), coinciding with Bond et al.'s [7] Icelandic glass lithological zone. There are no iceberg releases from Iceland at the present day; Bond et al. [7] suggest that this region results from volcanic eruptions onto drifting ice. A discrete cluster 3 sample group lies offshore from the east Greenland Scoresby Sund region (Precambrian granites and Tertiary basalts) and may represent IRD.

Further cluster 3 samples occur around the Azores, Canaries/Madeira area, reflecting erosion of (titano)magnetite-rich, mid-ocean ridge and volcanics [35].

4.5. Cluster 6

The geographic distribution of cluster 6 is widespread (Fig. 17). Notably, however, most samples extending from the eastern Nordic Seas have strong memberships to this cluster. These samples coincide with the low-susceptibility/low-IRD region of the Greenland Sea previously noted by Pirrung et al. [4] and also resemble the IRD

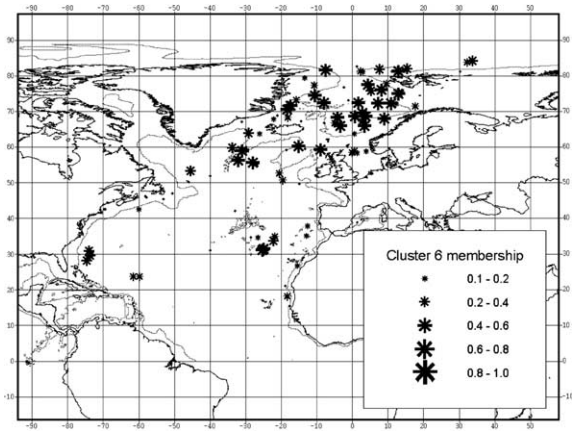

Fig. 17. Location of samples belonging to cluster 6. The symbol size represents the degree of affinity with the cluster.

area mapped (on the basis of >10% haematite-stained grains) by Bond et al. [7]. Smaller groups of samples occur off the Floridan coast, northwest of Africa, south of Iceland, north of Spitsbergen and along the eastern coast of Greenland. This cluster has a moderate χ_{ARM}/χ_{lf} mean value (17), χ_{fd} of 4%, HIRM of 5.7% and $IRM_{20\,mT}/IRM_{100\,mT}$ of 0.18. It appears to relate to areas where detrital inputs (from haematite-bearing IRD or dust) are relatively low at present. Some contribution from bacterial magnetite is also likely, given the low detrital supply.

4.6. Summary

Taking into account the cluster means, and the available source magnetic data, cluster 2 appears to reflect authigenic formation of bacterial magnetite, with no other significant detrital input. Clusters 5 and 9 represent aeolian dust. Clusters 1, 4, 7 and 8 are characterised by coarse-grained ferrimagnets. From comparison with present-day observations and iceberg model data [10,36], the majority of samples classified in these four clusters appear to contain IRD. Studies of glacial North Atlantic sediments have similarly shown that much of the IRD is associated with high concentrations of coarse-grained (MD and PSD) ferrimagnets with low coercivities and a 'soft' IRM signal [23,37–39]. Cluster 3 samples are also characterised by coarse ferrimagnets but their spatial distribution suggests they are more likely to be derived from mid-ocean ridge material or volcanic ash. The remaining cluster, 6, is geographically widespread but with a number of samples confined to the eastern half of the Nordic Seas; this cluster probably receives low inputs of haematite-bearing dust and/or IRD, coupled with some in situ formation of bacterial magnetite.

This interpretation of distinct sediment sources is supported by the NLM results (Fig. 11). Greatest interdata distance is apparent between the IRD-dominated sediments (clusters 1, 4, 7 and 8) and the bacterial magnetite (cluster 2) and dust clusters (5 and 9). Within the IRD clusters, 8 is separated from 1 and 4. Cluster 3 (mid-ocean ridge/volcanic) is less well separated from 7 (IRD and mid-ocean ridge mixed). Cluster 6 interfaces between clusters 3 and 7 and the dust and bacterial magnetite groupings. Subsequent runs of the cluster analysis were made, with the bacterial magnetite and the two dust sample groups removed, to assess if any further discrimination between the remaining clusters is possible. The best cluster solution in this case was six, with the spatial distribution and the magnetic parameter means matching closely those of the original analysis. This indicates both that no further discrimination is possible statistically and that the original nine-cluster solution is robust.

In summary, magnetic characterisation of present-day samples from across the North Atlantic, together with similar data for a range of potential sediment source areas, identifies distinct and statistically robust spatial groupings of sediment. These groupings in turn reflect mostly detrital inputs to the sediments, principally of IRD and windblown dust. These sediment transport pathways can be validated by making direct comparison of the sediment magnetic properties with source rocks and soils, and with iceberg trajectory and observation data. The spatial distribution of the IRD-dominated groupings suggest that deep water currents are less significant than previously proposed [6,40] in controlling present-day sediment mineralogy and distribution. Kissel et al. [6] identified little magnetic variation in sediment cores obtained along the trajectory of the

NADW, and on this basis proposed that such constancy could be explained by dominant bottom water transport of material from the Nordic basaltic province. However, the larger number of sediment samples analysed here presents a different picture, with several different statistical groupings occurring along this pathway (Fig. 12). This apparent contradiction may be explainable in that bottom water transport and deposition does occur – but is overshadowed magnetically wherever other detrital inputs (such as IRD) are supplied. Such an interpretation is independently supported by Prins et al.'s recent [41], particle size-based study which also identifies significant IRD inputs to areas previously thought dominated by ISOW flow.

In similar vein, in situ authigenesis of bacterial magnetite probably occurs over much of the ocean floor but is also only identified where detrital inputs are low.

5. Conclusions

Magnetic measurements of present-day, deep-sea sediments from across the North Atlantic identify distinct spatial patterns of sediment sources and transport pathways. Much of the sedimentary magnetic signal appears to be controlled by detrital inputs, especially of IRD and windblown dust. Sediments identified as having significant IRD inputs, which presently occur as far south as 40°N in the western North Atlantic, can be split statistically into four different clusters, reflecting different sources and/or mixing of sources. These IRD distributions can be compared explicitly with observational and iceberg trajectory data, and lithological tracer-based studies. They provide a present-day basis for comparison with glacial-stage IRD patterns and modes of ocean circulation (Watkins et al., in preparation). Previous studies have concluded that the magnetic signal of North Atlantic sediments along the NADW trajectory shows little variation, and that transport and deposition by bottom water is the dominant process. However, the larger data set shown here identifies significant input by IRD for discrete areas along this pathway.

In terms of windblown dust, the magnetic data delineate the source and spread of dust; statistical analysis identifies two, distinct westerly- and northwesterly-orientated dust 'plumes'. Again, these modern dust patterns can be used for comparison with previous glacial-stage distributions.

Authigenesis of magnetic material is only evident in those locations presently supplied with little detrital input. It is likely that bacterial magnetite is being formed across much of the North Atlantic at present but is overwhelmed magnetically by other, allochthonous inputs.

Finally, whilst magnetic discrimination of sediment sources and pathways seems effective for the majority of present-day samples, one statistical cluster (cluster 6) is notable by its rather wide geographic spread. It is likely that these sediments receive relatively small amounts of a mix of potential source materials at the present day.

Acknowledgements

This work was carried out under a Natural Environment Research Council PhD studentship (04/99/ES/62), jointly supervised by Dr Bigg at the University of East Anglia, and building on earlier discussions with Dr Robinson, Manchester University. We thank the following for access to deep-sea sediment samples: Dr Hardy, Canadian Geological Survey; Prof. Sarnthein, University of Kiel; Dr Rothwell, University of Southampton; Dr Smith, Scripps Institute of Oceanography; Dr Broda and Dr Roosen, Woods Hole Oceanographic Institute; Drs de Vernal and Bilodeau, University of Quebec at Montreal; Dr Matthiessen (Dr Pirrung, now at Jena), AWI-Bremerhaven; Prof. Andrews, INSTAAR, University of Colorado; and Dr Moros, University of Bergen. We thank the following for access to potential source samples: Drs Lavoie, Jackson and Frisch, Canadian Geological Survey; Dr Nakrem, University of Oslo; Dr Mcgarvie, Open University; Prof. Kent, Lamont-Doherty Earth Observatory; Dr Grimley, Illinois State Geological Survey; and Dr Hounslow, Lancaster University. Dr Dekkers (Utrecht) kindly made available the fuzzy cluster software.*[VC]*

Appendix. Magnetic instrumentation

Low-field, room-temperature and frequency-dependent susceptibility were measured using a dual frequency (0.46 kHz – χ_{lf} and 4.6 kHz – χ_{hf}) Bartington MS2B sensor, with frequency dependence calculated as:

$$\chi_{fd(\%)} = \frac{\chi_{lf} - \chi_{hf}}{\chi_{lf}} \times 100$$

To identify if the geographic distribution of susceptibility is influenced by carbonate content, a subset (60%) of susceptibility values were corrected for carbonate content, using the formula: $\chi_{lf} \times (1 - CO_3$ content (wt fraction)). Anhysteretic remanent magnetisation was imparted to samples using a Molspin AF demagnetiser, by placing them in a slowly decreasing alternating field from a peak of 80 mT. A superimposed DC field of 0.08 mT was applied parallel to the AC field and the resulting ARM was measured using a Molspin magnetometer. The ARM is expressed as a mass-specific susceptibility of ARM (χ_{arm}, 10^{-6} m^3 kg^{-1}) by normalising with the DC field:

$$\chi_{arm} = \frac{ARM}{f}$$

where ARM is the mass-specific ARM (10^{-4} Am^2 kg^{-1}) and f is the steady biasing field applied (in this case, 0.08 mT $\cong$ 63.66 Am^{-1}). ARMs were then demagnetised, before isothermal remanent magnetisations were measured (resulting from incrementally applied fields of 20, 100, 300 and 1000 mT), using a Molspin magnetometer. Fields from 20 to 300 mT were imparted using a pulse magnetiser and the 1 T ('saturation') field was imparted using a Highmoor DC electromagnet. The proportion of high field remanence acquired between 300 mT and 1 T, the HIRM%, was calculated as:

$$\%HIRM = \frac{SIRM - IRM_{300\,mT}}{SIRM} \times 100$$

References

[1] W.L. Balsam, F.W. McCoy, Atlantic sediments: glacial/interglacial comparisons, Paleoceanography 2 (1987) 531–542.

[2] W.L. Balsam, B.L. Otto-Bliesner, B.C. Deaton, Modern and last glacial maximum eolian sedimentation patterns in the Atlantic Ocean interpreted from sediment iron oxide content, Paleoceanography 10 (1995) 493–507.

[3] M. Cremer, F. Grousset, J.C. Faugeres, J. Duprat, E. Gonthier, Sediment flux patterns in the northeastern Atlantic – variability since the last interglacial, Mar. Geol. 104 (1992) 31–53.

[4] M. Pirrung, D. Futterer, H. Grobe, J. Matthiessen, F. Niessen, Magnetic susceptibility and ice-rafted debris in surface sediments of the Nordic Seas: implications for Isotope Stage 3 oscillations, Geo-Mar. Lett. 22 (2002) 1–11.

[5] F. Niessen, D. Weiel, Distribution of magnetic susceptibility on the Eurasian shelf and continental slope – implications for source areas of magnetic minerals, Rep. Polar Res. 212 (1996) 81–88.

[6] C. Kissel, C. Laj, L. Labeyrie, T. Dokken, A. Voelker, D. Blamart, Rapid climatic variations during marine isotopic stage 3: magnetic analysis of sediments from Nordic Seas and North Atlantic, Earth Planet. Sci. Lett. 171 (1999) 489–502.

[7] G. Bond, B. Kromer, J. Beer, R. Muscheler, M.N.. Evans, W. Showers, S. Hoffmann, R. Lotti-Bond, I. Hajdas, G. Bonani, Persistent solar influence on North Atlantic climate during the Holocene, Science 294 (2001) 2130–2136.

[8] K. Matsumoto, An iceberg drift and decay model to compute the ice-rafted debris and iceberg meltwater flux: Application to the interglacial North Atlantic, Paleoceanography 11 (1996) 729–742.

[9] J.A. Andrews, Icebergs and iceberg rafted detritus (IRD) in the North Atlantic: Facts and assumptions, Oceanography 13 (2000) 100–108.

[10] G.R. Bigg, M.R. Wadley, D.P. Stevens, J.A. Johnson, Prediction of iceberg trajectories for the North Atlantic and Arctic Oceans, Geophys. Res. Lett. 23 (1996) 587–3590.

[11] A.M. Schmidt, T. vonDobeneck, U. Bleil, Magnetic characterisation of Holocene sedimentation in the South Atlantic, Paleoceanography 14 (1999) 465–481.

[12] M. Hanesch, R. Scholger, M.J. Dekkers, The applications of fuzzy c-means cluster analysis and non-linear mapping to a soil data set for the detection of polluted sites, Phys. Chem. Earth 26 (2001) 885–891.

[13] P.P. Kruiver, Y.S. Kok, M.J. Dekkers, C.G. Langereis, C. Laj, A pseudo-Thellier relative palaeointensity record, and rock magnetic and geochemical parameters in relation to climate during the last 276 kyr in the Azores region, Geophys. J. Int. 136 (1999) 757–770.

[14] S.P. Vriend, P.F.M. van Gaans, J. Middelburg, A. Nus, The application of fuzzy c-means cluster analysis and non-linear mapping to geochemical datasets: examples from Portugal, Appl. Geochem. 3 (1988) 213–224.

[15] C.J. Bezdek, R. Ehrlich, W. Full, FCM: the fuzzy

c-means clustering algorithm, Comput. Geosci. 10 (1984) 191–203.
[16] J.W. Sammon, A nonlinear mapping data structure analysis, IEEE Trans. Comput. C18 (1969) 401–409.
[17] M.J. Dekkers, C.G. Langereis, S.P. Vriend, P.J.M. van Santvoort, G.J. de Lange, Fuzzy c-means cluster analysis of early diagenetic effects on natural remanent magnetisation acquisition in a 1.1 Myr piston core from the Central Mediterranean, Phys. Earth Planet. Inter. 85 (1994) 155–171.
[18] D.J.W. Piper, K.I. Skene, Latest Pleistocene ice-rafting events on the Scotian Margin (eastern Canada) and their relationship to Heinrich events, Paleoceanography 13 (1998) 205–214.
[19] B.A. Maher, Magnetic properties of some synthetic submicron magnetites, Geophys. J. 94 (1988) 83–96.
[20] J.A. Dearing, R.J.L. Dann, K. Hay, J.A. Lees, P.J. Loveland, B.A. Maher, K. O'Grady, Frequency-dependent susceptibility measurements of environmental materials, Geophys. J. Int. 124 (1996) 228–240.
[21] B.A. Maher, R. Thompson, M.W. Hounslow, Introduction, in: B.A. Maher, R. Thompson (Eds.), Quaternary Climates, Environments and Magnetism, Cambridge University Press, Cambridge, 1998, pp. 1–48.
[22] U. Schwertmann, R.M. Taylor, Iron oxides, in: J.B. Dixon, S.B. Weed (Eds.), Minerals in Soil Environments, Soil Science Society of America, Madison, WI, 1987, pp.
[23] S.G. Robinson, The Late Pleistocene palaeoclimatic record of North Atlantic deep-sea sediments revealed by mineral magnetic measurements, Phys. Earth Planet. Inter. 42 (1986) 22–47.
[24] B.A. Maher, P.F. Dennis, Evidence against dust-mediated control of glacial-interglacial changes in atmospheric CO_2, Nature 411 (2001) 176–180.
[25] G.C. Bond, R. Lotti, Iceberg discharges into the North Atlantic on millennial time scales during the last glaciation, Science 267 (1995) 1005–1010.
[26] P.E. Olsen, D.V. Kent, Long-period Milankovitch cycles from the Late Triassic and Early Jurassic of eastern North America and their implications for the calibration of the Early Mesozoic time-scale and the long-term behaviour of the planets, Phil. Trans. R. Soc. London A357 (1999) 1761–1786.
[27] Ö. Özdemir, S.K. Banerjee, A preliminary magnetic study of soil samples from west-central Minnesota, Earth Planet. Sci. Lett. 59 (1982) 393–403.
[28] N. Petersen, T. von Dobeneck, H. Vali, Fossil bacterial magnetite in deep-sea sediments from the South Atlantic Ocean, Nature 320 (1986) 611–615.
[29] P. Hesse, J.F. Stolz, Bacterial magnetite and the Quaternary record, in: B.A. Maher, R. Thompson (Eds.), Quaternary Climates, Environments and Magnetism, Cambridge University Press, Cambridge, 1998, pp. 163–199.
[30] D.F. McNeill, Biogenic magnetite from surface Holocene carbonate sediments, Great Bahama Bank, J. Geophys. Res. 95 (1990) 4363–4371.
[31] B.A. Maher, R.M. Taylor, Formation of ultrafine-grained magnetite in soils, Nature 336 (1988) 368–370.
[32] B. Moskowitz, R.B. Frankel, D.A. Bazylinski, Rock magnetic criteria for the detection of biogenic magnetite, Earth Planet. Sci. Lett. 120 (1993) 283–300.
[33] J.S. Stoner, J.T. Andrews, The North Atlantic as a Quaternary magnetic archive, in: B.A. Maher, R. Thompson (Eds.), Quaternary Climates, Environments and Magnetism, Cambridge University Press, Cambridge, 1999, pp. 49–80.
[34] NSIDC, International Ice Patrol (IIP) Iceberg Sightings Database, National Snow and Ice Data Center/World Data Center for Glaciology, Boulder, CO, 1995, digital media.
[35] S.G. Robinson, J.T.S. Sahota, F. Oldfield, Early diagenesis in North Atlantic abyssal plain sediments characterized by rock-magnetic and geochemical indices, Mar. Geol. 163 (2000) 77–107.
[36] G.R. Bigg, M.R. Wadley, D.P. Stevens, J.A. Johnson, Modelling the dynamics and thermodynamics of icebergs, Cold Reg. Sci. Technol. 26 (1997) 113–135.
[37] J. Bloemendal, J.W. King, F.R. Hall, S.-J. Doh, Rock magnetism of Late Neogene and Pleistocene deep-sea sediments: Relationship to sediment source, diagenetic processes and sediment lithology, J. Geophys. Res. 97 (1992) 4361–4375.
[38] F.E. Grousset, L. Labeyrie, J.A. Sinko, M. Cremer, G. Bond, J. Duprat, E. Cortijo, S. Huon, Patterns of ice-rafted detritus in the glacial North Atlantic (40–55N), Paleoceanography 8 (1993) 175–192.
[39] S.G. Robinson, M.A. Maslin, I.N. McCave, Magnetic susceptibility variations in Upper Pleistocene deep-sea sediments of the NE Atlantic: implications for ice rafting and paleocirculation at the last glacial maximum, Paleoceanography 10 (1995) 221–250.
[40] T.M. Dokken, E. Jansen, Rapid changes in the mechanism of ocean convection during the last glacial period, Nature 401 (1999) 458–461.
[41] M.A. Prins, L.M. Bouwer, C.J. Beets, S.R. Troelstra, G.J. Weltje, R.W. Kruk, A. Kuijpers, P.Z. Vroon, Ocean circulation and iceberg discharge in the glacial North Atlantic: Inferences from unmixing of sediment size distributions, Geology 30 (2002) 555–558.